# MODELING OF EFFECTIVE ELASTIC PROPERTIES OF CARBON/CARBON LAMINATES

Piat R., Böhlke T.
Institute of Engineering Mechanics, University of Karlsruhe (TH),
Kaiserstr. 10, D-76131 Karlsruhe, Germany
Romana.Piat@kit.edu

Dietrich S., Gebert J.-M., Wanner A.
Institute of Materials Science and Engineering I, University of Karlsruhe (TH),
Kaiserstr. 12, D-76131 Karlsruhe, Germany

## SUMMARY

Three-dimensional structural information obtained by X-ray computed tomography on carbon/carbon laminates is used as input for a mechanical model describing the elastic behavior of the composite. The model is based on a homogenization procedure consisting of three sequential steps covering the fiber and matrix interaction, the pores, and the laminate structure.

*Keywords: carbon/carbon composites, effective material properties, homogenization, micromechanics, microstructure modeling*

## INTRODUCTION

Carbon/carbon (C/C) composites fabricated by chemical vapor infiltration (CVI) of carbon fiber preforms have a complicated hierarchical microstructure [1, 2]. In this material, carbon fibers are embedded in a matrix of pyrolytic carbon (PyC), which has a cylindrically layered structure. The microstructure of the PyC matrix is strongly influenced by the CVI parameters (temperature, pressure, residence time and other), see [3, 4] for more information on CVI infiltration of the considered C/C materials.

Material properties of C/C composites on different length scales are difficult to identify because of the strong anisotropy of carbon fibers and PyC-matrix on the micrometer scale. The experimental measurements of the elastic properties of the PyC were conducted in [5, 6] using nanoindentation. However, it was assumed that PyC is isotropic and homogeneous, thus only the effective E-modulus of the PyC was obtained. Material properties of C/Cs on a macro scale were studied for different fiber architectures and, furthermore, different porosities and experimental studies by [7] provide useful information of the influence of the effect of void fraction on the flexural strength and modulus. An analytical modeling approach for predicting the stiffness of 3D orthotropic composites was developed in [8]. Hatta and his group performed a comprehensive experimental study on 2D and 3D composites [9-12] to analyze their strength in tension, shear and compression tests. Casal et al. [13] addressed the influence of porosity on the shear strength of the composite.

In our previous studies we have reported a microstructure modeling on different length scales. Higher-order bounds of textured PyC were predicted in [14] using the material properties of high textured (HT) PyC produced by Schunk Kohlenstofftechnik GmbH

and measured by combination of ultrasonic studies and three-point bending investigations [15]. The effective elastic response of the composites containing unidirectional (UD) and randomly-oriented fibers was discussed in [16-18].

In the present study, the PyC layers are modeled using a methodology proposed in [14] with the material properties of PyC [15]. The elastic properties of the entire composite are calculated using a homogenization procedure. The derived macroscopic effective properties are verified using macroscopic values obtained from experimental studies [18] and recent measurements [19].

## MATERIAL CHARACTERIZATION

One of the fabrication methods of C/C composites is the production by CVI. This process consists of a synthesis of carbon particles from hydrocarbon gas and their deposition on carbon fibers. CVI takes place in a hermetically closed high temperature reactor. Materials studied in this paper were produced during isothermal, isobaric CVI, and the process was performed at a constant temperature range of 1095°-1200°C and under pressures of 10-30 kPa.

The infiltration was carried out at the Institute for Chemical Technology of the University of Karlsruhe (TH). Other details about the infiltration procedure are given in [3, 4].

The microstructural architecture of C/Cs depends on the fiber orientation in the preform. Consequently, it is possible to obtain different materials: from UD orientation of the fibers (all fibers are oriented in one direction) to an infiltrated felt with random distribution of fibers. All these materials have a certain porosity, the pore distribution and shape are dependent on the preform structure, and the porosity can be controlled through the infiltration time. The fiber distribution in the preform already determines the architecture of the composite and, consequently, the effective mechanical properties.

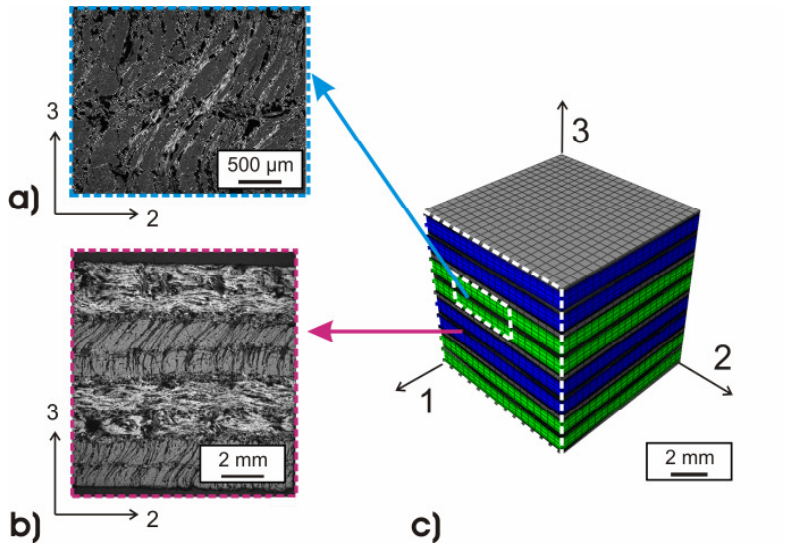


Figure 1: Typical microstructure of the material with 2D preform: micrographs of the microstructure of the composite a) local presentation of two UD layers separated by felt; b) material consisting of eight UD layers separated by felt; c) schematic presentation of the modelled laminate. Colours present (green and blue) different oriented UD layers and felt (grey-black).

In this paper, our studies focus on the analysis of materials with so called “2D preform”. The schema of the microstructure of these materials is presented in Fig. 1c. The fiber preform of these materials shows a laminate microstructure with a sequence of layers with UD fiber orientation separated by quite thin layers of the felt (grey layers in Fig. 1 c). The UD layers have two different perpendicular preferred orientations (see Fig. 1c: blue and green layers)). The entire composite is needled by some fibers perpendicular to UD orientations (direction 3 in Fig. 1c). Micrographs of the local microstructure of layers with one preferred orientation separated by a felt layer as well as micrographs of an analyzed part of laminated microstructure are presented on Fig. 1a and 1b.

**Characterization of the fiber distribution**

Firstly, we study the fiber distribution in the material. The three dimensional distribution of fibers can be determined by a micro computer tomographic (μCT) analysis. A cylindrical specimen of the non infiltrated preform was manufactured via water cutting and analyzed in a Desktop CT Scanner (Skyscan 1072). Our studies show that fiber bundles are oriented either parallel to the 1-axes or parallel to the 2-axes. Based on studies provided in [20], the volume fractions of the fibers in UD and felt layers can be calculated and thus corresponding to 10% and 23% of the fibers volume fraction. To further analyse the preferred orientation of carbon fibers, each voxel (2.9 μm) corresponding to a fiber was assigned to one of the three axes of the coordinate system (123). Therefore, an anisotropic Gaussian filter was applied with pronounced axes parallel to the 1-, 2- or 3-axes. The voxel was then assigned to the direction with the highest probability. The results of provided measurements show, that a nearly constant amount of 30 % of the fibers is oriented preferentially parallel to the 3-axes. 60 % of the fibers are oriented parallel to the direction of reinforcement (1- or 2-axes, depending on the layer) and the remaining 10 % are oriented perpendicularly to the above axes.

**Characterization of the pores distribution**

Secondly, we characterize the pores distribution in the C/C composite. In these studies we distinguish two different parts of the material microstructures: UD layers and layers with felt.

**The characterization of the pore distribution in UD layers** was provided using μCT analysis. The following procedure was carried out for each UD layer (Fig. 2):

- Each layer was extracted from the μCT Data and segmented into pores and material with a region growing algorithm;
- The pores were labelled and analyzed in the following procedure (if the pore volume exceeded a minimum volume of 20 voxels):

1. The pore surface was extracted as a point cloud;
2. An ellipsoid with the same volume as the pore under consideration was fitted with a principle component analyses;
3. The Euler angles, principle half axes and the volume of the pore were tabulated.

Using the described procedure, the information about porosity of the unidirectional layers was gathered. All obtained pores were approximated as oblate and prolate spheroids. The distribution of the half-axis ratio of the spheroids and corresponding volume ratio are presented in Fig. 3. The orientation of the spheroid is defined through

the orientation of their third semi-diameter, non equal to two other semi-diameters. Statistical studies show, that we mainly have prolate pores (Fig. 3c) with preferred orientation coinciding with preferred orientation of the UD fibers (see Fig. 3a, 3d). The oblate pores, which are characterized through the orientation of the short semi-axis, are randomly distributed around the fibers with the circle surface, characterized by large half- axes, with preferred orientation coinciding with fibers orientation (see Fig. 3b, 3d).

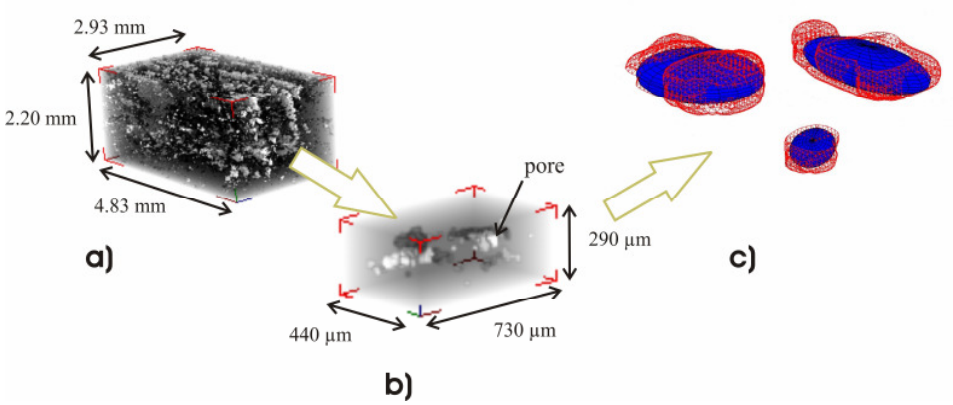


Figure 2: a) 3D images of the specimen part obtained from µCT; b) 3D images of the single pores; c) approximation of the pore structure within uni directional layers by ellipsoids with the same volume (the principle component analysis was used to fit the ellipsoids).

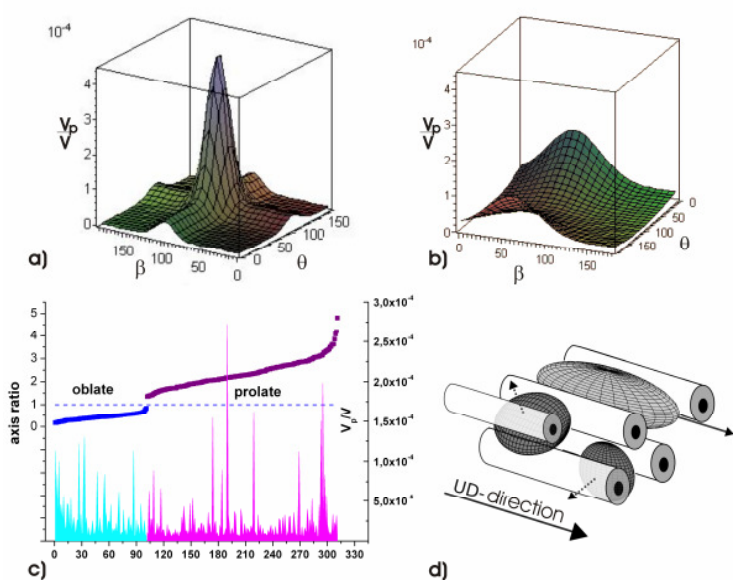


Figure 3: Porosity analysis in UD layers: Orientation distribution functions for a) prolate spheroids; b) oblate spheroids; c) distribution of axis and volume ratio for prolate and oblate spheroids; d) schematic presentation of the preferred orientations of prolate and oblate pores.

Methods for porosity studies for infiltrated felt were presented in our previous publications [17, 18, 21]. These methods are applied in the present study. They provide all necessary information for the modeling of the different layers and entire composite microstructure, and can be used directly for numerical studies.

## MATERIAL MODELING

For the prediction of the effective elastic properties of C/C laminates, we propose a three-step homogenization scheme:
1. We homogenize the material consisting of the pyrolytic carbon matrix with randomly distributed carbon fibers (for felt) or unidirectional fibers (for UD layers);
2. We embed the pores in the homogenized material obtained from the previous homogenization step. The pore morphology, i.e., the distribution of pore size and orientation is taken from μCT or metallographic microstructure studies;
3. The effective behavior of the laminate structure is determined in the third step using the FE-method.
In our studies, the modeling of the UD layers and felt-layers are provided separately.

**Modeling of UD layers.** For the first step of the homogenization of unidirectional fibers and PyC matrix the non-interaction schema can be used as presented in [22, 23], and the Mori-Tanaka homogenization schema for transversal isotropic matrix with transversal isotropic ellipsoidal inclusion can be used for a more accurate calculation of the effective material properties [23].

The microstructure studies show that the long axis of the prolate pores as also the circle cross-section of the oblate spheroids coincides with the fibres direction (Fig. 3a, 3b, 3d). A statistical study of the distribution of the axis ratios shows also that there aren't any spherical pores (Fig. 3c). For this reason, our problem can be approximated as 2D problems for materials with long pores [16].

For the calculation of the effective properties of the UD layer with pores two different methods can be used:

1. An approximation of the 3D-problem through a 2D problem. In this case, we can use our previous results for two dimensional composites. For irregular pore shapes, the exact shape functions can be used and the exact 2D solution, typical for C/C composites pores, can be found [16].

2. An approximation of the three dimensional pores as prolate and oblate spheroids and solution of the problem for three dimensional ellipsoidal pores in transversal isotropic material. In this case, the symmetry axes of the material coincide with the direction of the axis of the ellipsoidal pores. The statistical studies show that preferred orientation of the pores fulfils this condition. Then, the compliance contribution tensor **H** of the pore can be calculated using following formulae [23]:

oblate pore: $H_{ijkl} = f_p\left(h_5 T^5_{ijkl} + h_6 T^6_{ijkl}\right)$,

$$h_5 = \frac{64}{3\sqrt{2}C_5^0}\left[\sqrt{\frac{C_2^0}{C_5^0}} + \frac{-4\left(C_3^0\right)^2 + 2C_6^0\left(2C_1^0 + C_2^0\right)}{C_5^0\left(\sqrt{A_2}+\sqrt{A_3}\right)\sqrt{C_6^0\left(2C_1^0 + C_2^0\right)}}\right]^{-1},\ h_6 = \frac{8}{3}\frac{\left(\sqrt{A_2}+\sqrt{A_3}\right)\left(2C_1^0 + C_2^0\right)}{C_6^0\left(2C_1^0 + C_2^0\right) - 2\left(C_3^0\right)^2}, \quad (1)$$

and prolate pore: $H_{ijkl} = f_p \sum_\alpha h_\alpha T^{(\alpha)}_{ijkl}$

$$h_1 = \frac{2C_3^0C_4^0 - C_6^0\left(2C_1^0 + C_2^0\right)}{4C_2^0\left(C_3^0C_4^0 - C_1^0C_6^0\right)};\ h_2 = \left(\frac{1}{C_1^0} + \frac{2}{C_2^0}\right);\ h_3 = \frac{C_3^0}{2\left(C_3^0C_4^0 - C_1^0C_6^0\right)} \quad (2)$$

$$h_4 = \frac{C_3^0}{2\left(C_3^0 C_4^0 - C_1^0 C_6^0\right)};\ h_5 = \frac{8}{C_5^0};\ h_6 = \frac{C_1^0}{C_1^0 C_6^0 - C_3^0 C_4^0},$$

with $f_p$ being the volume fracture of the pores, $T_{ijkl}^{\alpha}$ are the components of ''standard'' tensorial basis (Tensorial basis in the space of transversely isotropic fourth rank tensors: [24].) and $C_j^0$ can be presented through components of the stiffness tensors of the material from the previous homogenization step:

$$C_1^0 = 0.5(C_{1111}^0 + C_{1122}^0), C_2^0 = 2C_{1212}^0, C_3^0 = C_{1133}^0, C_4^0 = C_{3311}^0, C_5^0 = 4C_{1313}^0, C_6^0 = C_{3333}^0. \quad (3)$$

The effective compliance $S_{ijkl}^{eff}$ of the composite with pores can be calculated using the non-interaction approximation:

$$S_{ijkl}^{eff} = S_{ijkl}^0 + H_{ijkl}^{NI},\ H_{ijkl}^{NI} = \sum H_{ijkl}^{p} \qquad (4)$$

$H_{ijkl}^{p}$ are the components of the compliance tensor of the pore p, which are calculated using (1) for oblate or (2) for prolate pores corresponding. $S_{ijkl}^0$ are the components of the compliance tensor of the material from the previous homogenization step

**Modeling of the felt.** The modeling of the felt was described in [17, 18, 21]. Firstly, we homogenize material consisting of PyC matrix and randomly distributed carbon fibers. Carbon fibers are approximated by randomly oriented needle-shaped inclusions. Using the Mori-Tanaka, the approximation of the compliance tensor of the material without pores can be calculated. The next step of the homogenization procedure is to insert the pores in the homogenized material of the previous step consisting of pyrolytic carbon matrix and fibers. Results presented in [18] show that calculations provided for oblate and prolate ellipsoidal pores give the upper and lower bounds of elastic properties of the composite which are sufficiently close to each other. Material properties calculated by an approximation based on a spherical geometry of the pores lie between these bounds and are close to the experimental values. This result allows for simplifying our calculations and we can use the Mori-Tanaka model which gives a good approximation for larger volume fractions of pores.

**Laminate modeling.** The next step for the calculation of effective material parameters of the whole composite is the modeling of the laminate by using the FE-method. An ABAQUS model was used to calculate the effective elastic constants of the laminate. The geometry of the model is presented in Fig. 1c. The model consists of 56000 elements (element type C3D8), eight solid sections, and two different materials (felt and UD). Six loading cases were applied with periodic displacement boundary conditions [25]. The corresponding stress components were weighted with the volume fraction of the element, and summed over the entire volume. The effective stiffness matrix was calculated from the global stress-global strain relation.

## NUMERICAL RESULTS AND EXPERIMENTAL VERIFICATION

As input values for our calculations, we use the measured transversal isotropic material properties of the PyC [15]. In our theoretical studies, we have separately modeled two different materials: infiltrated felt and UD layers. Overall response of the PyC-matrix in these two materials is different. The effective response of the PyC-matrix around the

fibers in the infiltrated felt is isotropic, and we need to obtain the effective isotropic properties of the PyC-matrix. For these calculations, we use our previous result [14, 26] with $E$=15.9 GPa and $\nu$=0.395. In case of the UD composites, the overall response of PyC is transversal isotropic und for the following calculations we use results obtained in [27] with $C_{1111} = 25.27, C_{3333} = 39.15, C_{1122} = 20.61, C_{1133} = 21.78, C_{1212} = 3.24$ [GPa].

Firstly, the material properties of the infiltrated felt were calculated. The effective Young's modulus obtained was compared with experimentally obtained ones. Three infiltrated felt materials with different porosity were tested (porosities see Table1): one of these materials (Felt1) by the tensile, and two others (Felt2 and Felt3) by four points bending tests. The results of these measurements of the mean values of Young's modulus, as well as the numerical results are presented in Table 1. Analyzing these results, we can conclude that the calculated material properties show good correspondence with the experimental data.

Table 1: Calculated and experimental values [19, 25] of Young's modulus of felt composite with different porosities and of laminate with UD layers with only one preferred orientation.

| | Volume of the fibers (%) | Volume of the pores (%) | Calculated Young's modulus [GPa] | Measured Young's modulus [GPa] |
|---|---|---|---|---|
| Felt1 | 12 | 7.3 | 18.18 | 18.6 |
| Felt2 | 12 | 15 | 16.432 | 16.6 |
| Felt3 | 12 | 48 | 13.069 | 12.4 |
| Laminate1 | 23 in UD part<br>10 in felt part | 9 in UD part<br>20 in felt part | 49.94 | 51, Ref.[16] |

Secondly, the material properties of the laminate with UD layers in one preferred orientation separated through thin felt layers were calculated (Table1 results for Laminate1).

The calculated effective Young's modulus of this material was compared with the experimental one obtained by tensile tests (see the results of Table 1 for Laminate1).

Thirdly, the material properties of the laminate (Laminate2) consisting of eight UD layers (four UD layers oriented parallel to direction 1 and four parallel to direction 2). The effective properties of the composite were calculated.

For the verification of the numerical results for Laminate1 and Laminate2, the effective elastic constants were measured via Ultrasound Phase Spectroscopy (UPS) [28]. Using this method, two samples were studied. One of these samples consists of material from Laminat1 (two UD layers which are oriented parallel to direction 1) and the second one from Laminate2 (8 UD Layers, separated by thin layers of felt, see Fig. 1c). For more information about the geometry and density of these samples see Table 2.

Table 2: Samples investigated via Ultrasound Phase Spectroscopy (UPS).

| | | Density (g/cm³) | L1 (mm) | L2 (mm) | L3 (mm) |
|---|---|---|---|---|---|
| Laminate1 | 2 UD Layers | 1.70 | 10.46 | 10.43 | 2.30 |
| Laminate2 | 8 UD Layers | 1.69 | 10.45 | 10.46 | 10.46 |

The measurements were conducted in a frequency range of 10 kHz up to 8 MHz depending on the type of ultrasound transducer used, and the sample attenuation. The results of these measurements are presented in Fig. 4a for Laminate1 and Fig. 4b for Laminate2. It can be seen, that for both samples the direction 3 (perpendicular to the layers) shows non-dispersive wave propagation with a velocity of 3300 m/s (Laminate1) and 2300 m/s (Laminate2). Laminate2 shows a frequency dependence of the wave velocity for the in-plane directions. For frequencies above 1 MHz the wave propagation is most probably dominated by UD layers oriented parallel to the direction of propagation and the measured velocity does not represent the effective material response.

For comparing of the numerical and experimental values obtained via UPS the numerical effective elastic properties we recalculated in corresponding wave propagation [28, 29]. Obtained values are presented as arrows in Fig. 4. The calculated velocities are quite close to the measured velocities.

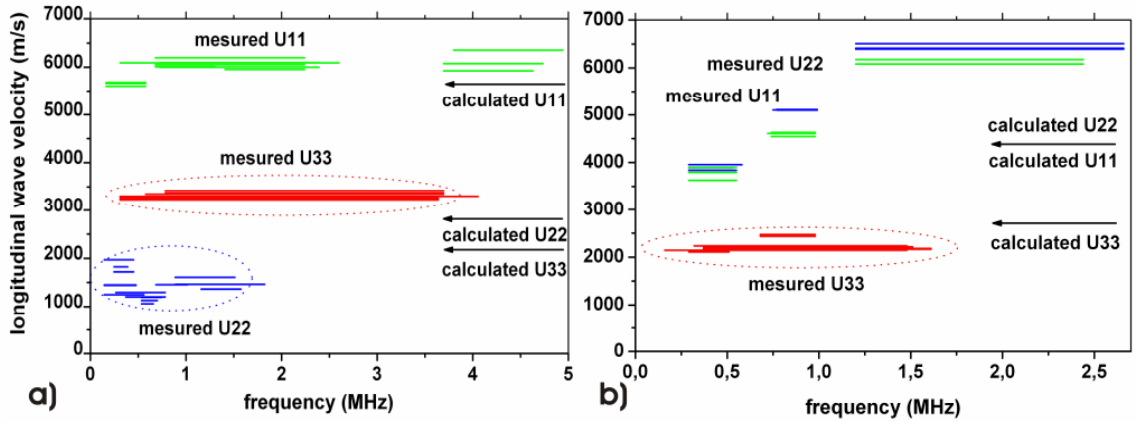


Figure 4: Measured and calculated waves velocities for a) Laminate1 and b) Laminate2.

## CONCLUSIONS

The characterization, modeling and experimental verification procedure is presented for the calculation of effective material properties of C/Cs laminates. This procedure consists of fibers and pores distributions characterization using µCT, followed by consequential steps of the microstructure homogenization. Prediction of the material parameters of the UD layers and felt-layers are provided separately. For each of these layers, firstly the effective material properties of the fibers and PyC-matrix are calculated, and secondly the pores are embedded in effective material from the first

homogenization step. The obtained effective parameters of the layers are used for the calculation of the effective material properties of the entire laminate using the FE-model.

The verification of the numerical modeling is provided using experimental methods for different layers and for the whole laminate.

The following comparisons of the numerical and experimental results for the testing of the samples with the same material microstructure as in the model are provided:

1. Young's modulus of the infiltrated felt with different porosities was compared with the one obtained by mechanical testing;

2. The effective stiffness of the laminate with UD layers in one preferred orientation separated through thin felt layers was compared with the results of tensile tests and UPS measurements;

3. The effective stiffness of the whole laminate was compared with UPS measurements.

The comparison shows that using the proposed homogenization procedure, it is possible to provide good prediction of the overall material properties of the composite.

The proposed method provides a methodology to predict the effective material properties of C/C materials based on the information on their microstructure and volume fractions of the micro constituents. The utilization of this method allows for reducing the volume of experimental mechanical tests, and also opens a perspective to provide numerical optimization of C/C composites to obtain the required material behaviour.

## ACKNOWLEDGEMENTS

The authors thank the Institute for Chemical Technology and Polymer Chemistry (O. Deutschmann) at the University of Karlsruhe (TH), Germany for providing the C/C material and Prof. I. Tsukrov (University of New Hampshire, USA) for the interesting and useful discussions on the concept of homogenization. The financial support of the DFG (NSF-DFG Project: “Materials World Network: Multi-Scale Study of Chemical Vapor Infiltrated C/C Composites”, BO 1466/3-1; the Heisenberg fellowship (DFG PI 785/1-1) and the collaborative research centre 551 “Carbon from the gas phase: elementary reactions, structures and materials”) is gratefully acknowledged.

## References

1. B. Reznik, G. Gerthsen, KJ. Hüttinger, Carbon **39**(2001) 215-229.
2. R. Piat, E. Schnack, Carbon **41**(2003) 2121-2129.
3. W. Benzinger, KJ. Hüttinger, Carbon **37**(1999) 941-946.
4. W. Benzinger, KJ. Hüttinger, Carbon **37**(1999) 1311-1322.
5. G. Hofmann , M. Wiedenmeier , M. Freund , A. Beavan , J. Hay , G.M. Pharr, Carbon **38**(2000) 645-653.
6. C.A. Taylor, M.F. Wayne, W.K.S. Chiu, Thin Solid Films **429**(2003) 190-200.
7. Z. J. Wu, D. Brown, J.M. Davies, Compos. Struc. **56**(2002) 407-412.
8. SS. Tzeng, JN. Pan, Mat. Sci. and Eng. **316a** (2001) 127-134.

9. H. Hatta, K. Goto, S. Ikegaki, I. Kawahara, M. Aly-Hassan, H. Hamada, J. of Eur. Cer. Soc. **25**(2005) 535-542.

10. M. Aly-Hassan, H. Hatta, S. Wakayama, M., Watanabe, K. Miyagawa, Carbon **41**(2003) 1069-1078.

11. H. Hatta, K. Suzuki, T.Shigei, T. Somiya, Y. Sawada, Carbon **39**(2001) 83-90.

12. H. Hatta, K. Goto, T. Aoki, Comp. Sci. and Tech. **65** (2005) 2550-2562.

13. E. Casal, M. Granda, J. Bermejo, J. Bonhomme, R. Menéndez, Carbon **39**(2001) 73-82.

14. T. Böhlke, T.-A. Langhoff, R. Piat, PAMM submitted.

15. B. Viering, J.-M. Gebert, A. Wanner, unpublished, Institut für Werkstoffkunde I, Universität Karlsruhe (TH), 2007.

16. I. Tsukrov, R. Piat, I. Novak, E. Schnack, Mech. of Adv. Mat. & Struc. **12**(2005) 43-54.

17. R. Piat, N. Mladenov, I. Tsukrov, V. Verijenko, M. Guellali, E. Schnack, MJ. Hoffmann, Comp. Sci. and Tech. **66**(2006) 2997-3003

18. R. Piat, N. Mladenov, I. Tsukrov, M. Guellali, R. Ermel, T. Beck, E. Schnack, MJ. Hoffmann, Comp. Sci. and Tech. **66**(2006) 2769-2775.

19. A. Bussiba, R. Piat, T. Böhlke, R. Carmi, I. Alon, M. Kupiec, Ref. Nr.817. Carbon 2009, Biarritz, France, June 14-19, 2009.

20. T. Chen, B. Reznik, D. Gerthsen, W.Zhang, K. Hüttinger, Carbon **43** (2005) 3088–3098.

21. J.-M. Gebert, A. Wanner, R. Piat, M. Guichard, S. Rieck, B. Paluszynski, T. Böhlke, Mech. of Adv. Mat. and Struct. **15** (2008) 467 -473.

22. M. Kachanov, B. Shafiro, I.Tsukrov, Handbook of elasticity solutions. Kluwer academic publishers, 2004.

23. I. Sevostianov, N. Yilmaz, V. Kushch, V. Leviv, Int. J. of Solids and Str. **42** (2005) 455-476.

24. I.A. Kunin, Elastic Media with Microstructure. Springer, Berlin, 1983.

25. K. Xu, X. W. Xu, Mat. Sci. and Eng. A, **487** (2008) 499-509.

26. R. Piat; T. Böhlke, I. Tsukrov, B. Reznik, O. Deutschmann, A. Bussiba, Ref.Nr.597, Carbon 2009, France, June 14-19, 2009.

27. S. Dietrich, J.-M. Gebert, A. Wanner, unpublished, Institut für Werkstoffkunde I, Universität Karlsruhe (TH), 2008.

28. A. Wanner, Mat. Sci. and Eng. A, **248** (1998) 35–43.

29. W.G. Zhang, K.J. Hüttinger, Carbon **41** (2003) 2325–2337.